

---

# Effects of Time Discrepancies Between Input and Myocardial Time-Activity Curves on Estimates of Regional Myocardial Perfusion with PET

Pilar Herrero, Judy J. Hartman, Martha J. Senneff and Steven R. Bergmann

*Cardiovascular Division, Washington University School of Medicine, St. Louis, Missouri*

---

Estimates of myocardial perfusion with PET using kinetic models require faithful recording of radioactivity content in blood and myocardium. Typically the arterial time-activity curve is obtained by placing a region of interest (ROIs) within the left atrial or left ventricular cavity. However, curves generated from these regions appear earlier in time than tissue time-activity curves obtained from ROIs within the myocardial tissue, and such time discrepancies can lead to errors in flow estimates. **Methods:** The magnitude of these time discrepancies and their effect on estimates of regional myocardial perfusion using oxygen-15-water were measured in 30 normal subjects evaluated at rest and again after administration of dipyridamole. **Results:** Under baseline conditions, the left atrial curve appeared  $0.97 \pm 0.67$  (s.d.) before the ascending aorta input curve ( $p < 0.05$ ) and estimated perfusion decreased from  $1.28 \pm 0.28$  ml/g/min using the left atrial curve uncorrected for time to  $0.98 \pm 0.27$  ml/g/min after correction ( $p < 0.05$ ). After dipyridamole, the left atrial curve appeared  $0.68 \pm 0.72$  sec before the ascending aorta curve ( $p < 0.05$ ) and estimated perfusion decreased from  $3.60 \pm 1.40$  ml/g/min using the left atrial curve uncorrected for time to  $3.24 \pm 1.26$  ml/g/min using the time-corrected curve ( $p < 0.05$ ). Because the magnitude of time discrepancies between the left ventricular and ascending aortic curves was less ( $0.25 \pm 0.34$  and  $0.19 \pm 0.23$  sec at rest and after dipyridamole, respectively), effects on flow estimates were more modest. **Conclusions:** The results of this study demonstrate that time discrepancies between input and tissue time-activity curves can affect estimates of myocardial flow. Correction for this potential source of error is proposed.

**Key Words:** PET; myocardial perfusion imaging

**J Nucl Med 1994; 35:558-566**

---

**N**oninvasive assessment of myocardial perfusion at rest and after stress is important for the objective evaluation of coronary vascular disease and for quantification of myo-

cardial perfusion reserve. PET has become a powerful tool for quantification of myocardial perfusion due to its ability to accurately delineate the distribution of positron-emitting radionuclides within the body. We and others have previously demonstrated that myocardial perfusion can be measured accurately with PET using radiolabeled oxygen-15-water ( $H_2^{15}O$ ) (1-6), nitrogen-13 ammonia ( $^{13}NH_3$ ) (7,8), rubidium-82-chloride ( $^{82}Rb$ ) (9-13), and, more recently, copper-62-pyruvaldehyde-bis-( $^4N$ -thiosemicarbazone) ( $^{62}Cu$ -PTSM) (14-16) using kinetic modeling when the input function (the history of tracer content with respect to time in the arterial blood perfusing the tissue bed of interest) and myocardial tissue activity are measured.

The accuracy and reliability of flow estimates depend on the accuracy of the measured input and tissue curves as well as on the physiological and mathematical appropriateness of the kinetic models used. For studies of myocardial perfusion, noninvasive measurement of the input curve can be obtained by placing a region of interest (ROI) on the reconstructed images within three regions: the left atrial cavity, the left ventricular cavity or within the ascending aorta. The ascending aorta is very close to the coronary ostia and is therefore the preferred location from which to obtain the input function for the myocardial bed. Nonetheless, accurate measurement of activity from this location is hampered by partial volume effects associated with the relatively small diameter of the ascending aorta with respect to the resolution of current tomographs and by potential contamination from tracer in other vascular structures (i.e., the pulmonary artery). Although most investigators generate the input function from a ROI placed within the left ventricular cavity (7,8,17,18), we have previously shown that generation of the input function from a ROI placed within the left atrial cavity is more accurate (2) since the left atrial cavity is not subject to as much motion artifact, has a larger physical dimension in the transaxial plane, and is subject to less spillover of radioactivity from myocardium than regions placed within the left ventricular cavity. These attributes are especially important for accu-

---

Received Mar. 29, 1993; revision accepted Sept. 15, 1993.  
For correspondence or reprints contact: Pilar Herrero, MS, Cardiovascular Division, Washington University School of Medicine, Box 8086, 660 S. Euclid Ave., St. Louis, MO 63110.

rate determinations of the input function when using extracted flow tracers.

Blood activity sampled noninvasively from regions placed within either the left atrial or left ventricular blood pool appear earlier in time than blood sampled from the ascending aorta. This results in a time offset between the input and tissue curves. Using computer simulations, we have previously shown that such time discrepancies can lead to errors in flow estimates and that such errors increase with decreasing flow levels (5).

Accordingly, the aims of the present study were: (1) to evaluate in human subjects the magnitude of the time differences between the input function obtained from either the left atrial or the left ventricular cavity compared with the input function obtained from the ascending aorta, (2) to assess the effect of these time differences on the flow estimates obtained, and (3) to implement a correction scheme for these time offsets when needed.

## METHODS

### Study Subjects

A group of 30 human volunteers consisting of 10 females and 20 males with a mean age of 44 yr (range 20–71 yr) were studied. Flow data from 24 of these subjects have been previously reported (19). All were without history or symptoms suggestive of coronary artery disease. Subjects refrained from oral intake of methylxanthines (including caffeine) for at least 12 hr prior to the study so the effects of dipyridamole would not be attenuated. Written informed consent was obtained. Twenty-four subjects were studied in Super PET I, a whole-body time-of-flight PET scanner that permits simultaneous acquisition of seven transaxial slices with a center-to-center slice separation of 1.5 cm, a slice thickness of 1.14 cm and a reconstructed resolution of 13.5 mm FWHM. The other six subjects were studied in Super PET 3000-E, a recently acquired, high count rate capability tomograph with a center-to-center slice separation of 1.42 cm, a slice thickness of 1.05 cm and a reconstructed resolution of 12 mm, FWHM (20).

### Tomographic Data Acquisition

After collection of attenuation data obtained with a transmission scan of the chest using an external ring or rod of germanium-68/gallium-68, 0.4 mCi/kg of  $H_2^{15}O$  was injected as a bolus (over 3–5 sec) through a large-bore catheter inserted into an antecubital vein. Data were collected in list mode beginning at the time of the initiation of the infusion for 100 sec. After a 10-min interval to allow activity of the tracer to decay to baseline levels ( $t_{1/2}$  of  $^{15}O = 2.0$  min), 40–50 mCi of  $^{15}O$ -labeled carbon monoxide ( $C^{15}O$ ) were administered by inhalation to label the blood pool. After a subsequent interval of 30–60 sec to allow clearance of CO from the lungs, data were collected for 5 min. After completion of data collection during baseline conditions, an intravenous infusion of 0.14 mg/kg per min over 4 min (0.56 mg/kg total dose) of dipyridamole was given (Persantine, Boehringer-Ingelheim, Ridgefield, Connecticut). After an interval of approximately 4 min to permit development of peak responses to dipyridamole, the tomographic imaging sequence was repeated.

### Analysis of Tomographic Data

Oxygen-15-labeled water data were reconstructed in two different ways. For use in visualizing the myocardium and assigning ROIs, a composite 100-sec image was reconstructed. For quanti-

fication of regional myocardial perfusion using a one-compartment kinetic model previously described and validated by us (2,5), data was reconstructed into 18, 5-sec frames. The  $C^{15}O$  tomographic data was also reconstructed into a single composite 300-sec image and was used for placing ROIs within the blood pool.

ROIs representing volumes of 1.65  $cm^3$  were placed within three different locations of the reconstructed  $C^{15}O$  image: the left atrial cavity, the left ventricular cavity and the ascending aorta. Two to four ROIs (representing volumes of approximately 5.0  $cm^3$ ) per ventricular slice were placed within anterior, septal, lateral and posterior myocardium on the composite  $H_2^{15}O$  image after correction for vascular radiolabeled water as described previously (2). Then, using the dynamic data, arterial blood and regional tissue time-activity curves were obtained from all ROIs.

Some protocols collect emission data for four or more min after either bolus or infusion administration of tracers. To evaluate whether shifts in the input function have varying effects on estimates of flow dependent on scan length, dynamic data from four patients with chest pain but angiographically normal coronary arteries were reconstructed after a single bolus administration of  $H_2^{15}O$  under resting conditions. Parameters were estimated using either the initial 90 sec of data or for 5.5 min. Data were formatted into eighteen 5-sec frames followed by fifteen 15-sec frames.

### Calculation of Time Differences

Time discrepancies between input curves obtained from regions placed within the left atrial and left ventricular cavities and that obtained from a ROI placed within the aortic root were estimated. Although there may be a slight delay in delivery of tracer from the ascending aorta into the myocardial tissue, it was assumed that the reference curve obtained from the aortic root was temporally aligned with myocardial tissue curves. The ascending aorta was sampled from a ROI placed approximately 1.4–2.8 cm above the base of the heart.

Estimates of time differences between the input and reference curve were obtained in each individual for each intervention (i.e., during baseline conditions and after dipyridamole) using a weighted linear least-squares curve fitting routine which estimates the time difference between the two curves by shifting the input curve towards the reference curve in increments of 0.1 sec and linearly interpolating the input curve. Then the weighted sum of the squares errors between the two curves is computed and the process of shifting and interpolating is repeated until a minimum sum of squares errors is obtained.

### Calculation of Myocardial Blood Flow from PET Data

Regional myocardial blood flow in ml/g/min was estimated using a one-compartment model which incorporates corrections for tissue partial volume and blood-to-tissue spillover effects as detailed previously (2,5). In the estimating process, data were weighted by the statistical noise of the activity in each tissue ROI by assuming that the variances of the experimental as well as of the fitted data were not negligible and that the undecay-corrected tissue activity data has a Poisson distribution. Flow was calculated for a given tissue region five different times. Flow in each tissue region was calculated using input functions generated from the left atrial and the left ventricular cavity without correction for time discrepancies. Then, flow was recalculated after shifting the left atrial and left ventricular input curves to temporally match the input curve obtained in the ascending aorta. In addition, flow in each region was calculated after shifting the left atrial curve to temporally match the left ventricular input curve. For each tissue

region and input function, individual region values of the tissue recovery coefficient ( $F_{MM}$ ) and the blood-to-tissue spillover fraction ( $F_{BM}$ ) were estimated along with estimates of flow within the operational flow equation.

For each subject and input function, mean flow,  $F_{MM}$  and  $F_{BM}$  for the whole heart were obtained by averaging all regional values. Regional variation in myocardial flow defined by the coefficient of variation of flow was calculated by dividing the standard deviation of regional flow values by the mean flow. Changes in parameter estimates as a function of time discrepancies were characterized using regression analysis.

### Measurement of Dispersion

Estimated time differences between either the left atrial or left ventricular curves and the ascending aorta curve would not be reliable if there are significant differences in dispersion of the blood activity sampled from these different locations. To evaluate whether significant dispersion between the left atrial and the ascending aorta curves occurred, a dispersion model was implemented in five studies (21,22). The model accounted for partial volume effects in the curve obtained from the aorta as well as for time discrepancies between the two curves. The dispersion coefficient ( $\tau$ ) averaged  $0.29 \pm 0.08$  sec, indicating negligible dispersion and suggesting that dispersal effects could be neglected.

To further evaluate the effect of dispersion on flow estimates as compared to the effect of input time shift on flow estimates, simulations were performed. The input function was defined by the gamma-variate function:

$$Ca(t) = 2000 t \exp(-t/tp), \quad \text{Eq. 1}$$

where  $tp = 5.0$  sec.

An analytical PET tissue curve for a flow of 1.0 ml/g/min,  $F_{MM}$  of 0.7, and  $F_{BM}$  of 0.2 was generated as detailed previously (5). To evaluate the effect of input time shift on flow estimates, the input curve was shifted 0.3, 0.6, 1.0 and 2.0 sec and the corresponding shifted function along with the generated PET tissue curve was used as input into the compartmental model. Estimated flow,  $F_{MM}$ , and  $F_{BM}$  values were compared to the modeled values for each of the time shifts.

To evaluate the effect of a dispersed input function on flow estimates, the analytical input function above was convolved with a dispersion function:

$$g(t) = \exp(-t/\tau)/\tau, \quad \text{Eq. 2}$$

where  $\tau$  = dispersion coefficient (sec) for  $\tau$  values of 0.3, 0.6, 1.0, and 2.0 sec. The corresponding dispersed input function along with the generated PET tissue curve was used as input into the compartmental model. Estimated flow,  $F_{MM}$  and  $F_{BM}$  values were compared to modeled values for each of the dispersed curves.

### Statistical Analysis

A two-way analysis of variance for repeated measures was used to compare differences in the estimated parameters due to different input functions. The two-way analysis accounted for two different sources of error: that due to the use of different input functions (LA and LV) and the systematic error due to the use of different time shifts with the same input. A two-way analysis of variance for repeated measurements was used to analyze differences in the estimated parameters due to different scan lengths. The analysis accounted for two different sources of error: that due to different scan lengths and the systematic error due to the use of

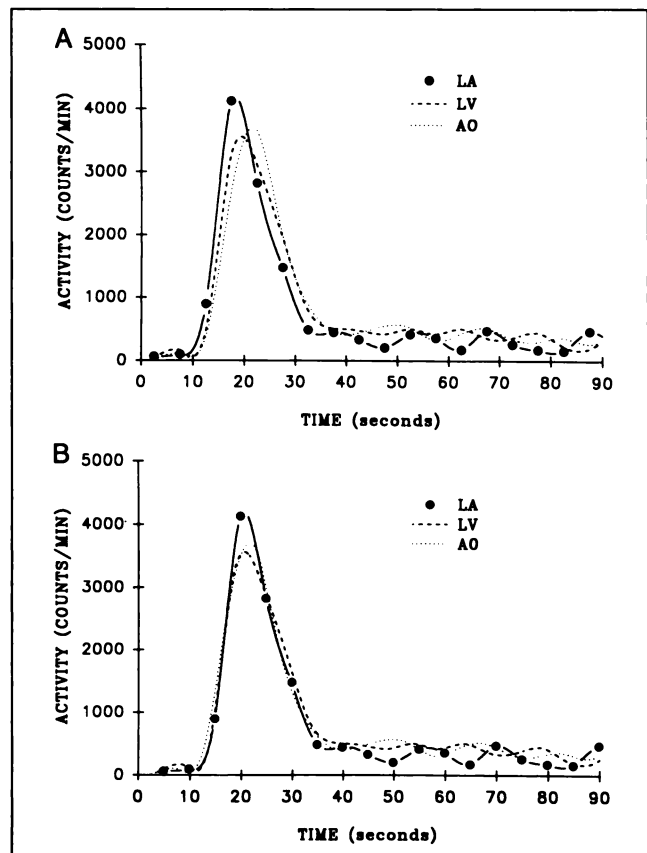


**FIGURE 1.** (A) Time-activity curves sampled from ROIs placed within the left atrial cavity (LA) (solid line), the left ventricular cavity (LV) (dashed line) and the ascending aorta (AO) (dotted line) from a subject studied under resting conditions. While the LA curve is sharper, has a higher peak activity than either the LV or the AO curves and shows decreased activity after 40 sec (i.e., is subjected to less partial volume and spillover effects), it appears earlier in time. (B) The same curves after the LA and LV curves were shifted in time to match the AO curve (2.3 and 1.2 sec, respectively). This striking example clearly shows the time differences among the three different input curves.

different time shifts. A p value less than 0.05 using the post hoc Scheffe test was considered statistically significant.

### RESULTS

A total of 202 myocardial ROIs were evaluated in the 30 subjects studied at rest, and 261 regions were evaluated after dipyridamole. ROIs were excluded from the analysis if the coefficient of variation of the flow parameter was greater than 50%. The use of this criterion allowed for the exclusion of statistically unreliable flow values.

### Time Discrepancies

As anticipated, the appearance of the input curve obtained from a region placed within the left atrial cavity temporally preceded the curves obtained from those in either the left ventricular chamber or the ascending aorta. Examples of input curves obtained from these regions and uncorrected with respect to time are shown in Figure 1A. Figure 1B demonstrates the curves after they had been

**TABLE 1**

Estimates of Time Discrepancies, Flow, Flow Variation, Partial Volume and Spillover Effects from 30 Volunteers Studied Under Conditions of Rest and After Dipyridamole

Input	Rest					Dipyridamole				
	Shift (sec)	MBF (ml/g/min)	COV (%)	F <sub>MM</sub>	F <sub>BM</sub>	Shift (sec)	MBF (ml/g/min)	COV (%)	F <sub>MM</sub>	F <sub>BM</sub>
LA	0.0	1.28 ± 0.28	20 ± 8	0.53 ± 0.12	0.25 ± 0.04	0.0	3.60 ± 1.40	23 ± 18	0.60 ± 0.10	0.23 ± 0.06
LA-AO	0.97 ± 0.67*	0.98 ± 0.27*	25 ± 10*	0.56 ± 0.17	0.29 ± 0.05*	0.68 ± 0.72*	3.27 ± 1.29*	22 ± 15	0.55 ± 0.09*	0.28 ± 0.07*
LA-LV	0.79 ± 0.43*	1.05 ± 0.23*	22 ± 7	0.53 ± 0.12	0.28 ± 0.04*	0.72 ± 0.57*	3.24 ± 1.26*	22 ± 11	0.54 ± 0.08*	0.29 ± 0.07*
LV	0.0	1.19 ± 0.44	25 ± 10	0.50 ± 0.11	0.29 ± 0.05	0.0	3.74 ± 1.52	23 ± 12	0.50 ± 0.08	0.27 ± 0.06
LV-AO	0.25 ± 0.34†	1.11 ± 0.46	26 ± 11	0.52 ± 0.14	0.30 ± 0.05	0.19 ± 0.23	3.61 ± 1.49	24 ± 11	0.47 ± 0.11	0.29 ± 0.08

\*p < 0.05 when compared to values obtained using the unshifted left atrial (LA) input.

†p < 0.05 when compared to values obtained using the unshifted left ventricular (LV) input.

Input = input function used; LA = left atrial cavity curve; LV = left ventricular cavity curve; LA-AO = left atrial curve shifted in time to match the ascending aorta curve; LA-LV = left atrial curve shifted in time to match the left ventricular curve; LV-AO = left ventricular curve shifted in time to match the ascending aorta curve; Shift = time shift between input and reference curve; F<sub>MM</sub> = tissue recovery coefficient; F<sub>BM</sub> = tissue-to-blood spillover fraction; MBF = myocardial blood flow; COV = regional coefficient of variation of flow. Values represent the mean ± s.d.

temporally aligned using the least-squares fitting routine. Peak activity in the curves obtained from the aorta and left ventricular cavity were diminished compared to the peak activity obtained in the left atrial curve, whereas the tail of the aorta and left ventricular curves were higher than that of the left atrial curve consistent with our previous observations (2) that activity obtained in the left atrial cavity is less contaminated by partial volume and spillover effects compared to activity obtained from either the left ventricular cavity or the ascending aorta.

Under baseline conditions, the input curve appeared an average of 0.97 ± 0.67 sec earlier in the left atrial cavity than in the ascending aorta (range 0.0–2.6 sec), and 0.79 ± 0.43 sec earlier than in the left ventricular cavity (range 0.0–1.7 sec) (p < 0.05 for each comparison, Table 1). The time delay between the input curve obtained from the left ventricular cavity compared to that obtained in the aorta was significantly shorter, 0.25 ± 0.34 sec (p < 0.05). During hyperemic conditions, the input curve appeared an average of 0.68 ± 0.72 sec earlier in the left atrial cavity than in the ascending aorta (range 0.0–3.2 sec), and 0.72 ± 0.57 sec earlier than in the left ventricular cavity (range 0.1–1.90 sec) (p < 0.05 for each comparison, Table 1, Fig. 2). Under hyperemic conditions, the time delay between the input curve from the left ventricular cavity compared to that obtained in the aorta averaged 0.19 ± 0.23 sec (range 0.0–1.1) (p = ns).

**Effects of Time Differences on Estimates of Myocardial Perfusion**

Mean flow estimated under resting conditions using the left atrial input uncorrected for its earlier appearance was significantly higher than flow obtained using the left atrial input shifted in time to match either the ascending aorta input or the left ventricular input (Table 1, Fig. 3A). Shifting the left ventricular input to match the ascending aorta input did not significantly alter flow estimates from those obtained using the nonshifted left ventricular input.

Figure 3B depicts the coefficient of variation of the resting flow estimates for each of the input functions used. The regional variation obtained using the left atrial input shifted in time to match the ascending aorta input was slightly higher than the variation obtained using either the left atrial input or the left atrial input shifted in time to match the left ventricular input but differences were modest.

Figure 4 depicts mean flow and the mean regional coefficient of variation of flow obtained under hyperemic conditions after intravenous dipyridamole. A similar trend to that observed for flows obtained under resting conditions was found although the magnitude of the effects was less since the time discrepancies were smaller with hyperemia.

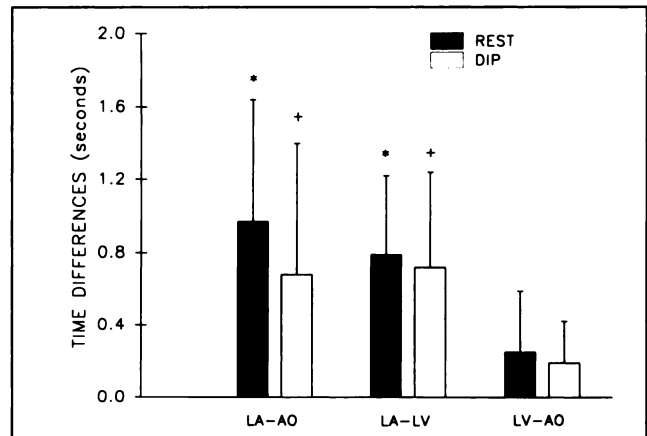


**FIGURE 2.** Estimates of time discrepancies between input functions at rest and after dipyridamole (dip). The time delays between the left atrial and ascending aorta curves (LA-AO) and between the left atrial and left ventricular curves (LA-LV) were significantly larger than time delays between the left ventricular and the ascending aorta curves (LV-AO) both at rest and after dipyridamole). Values in this and all subsequent graphs represent the mean ± s.d. \*p < 0.05 with respect to rest LV-AO, +p < 0.05 with respect to postdipyridamole (dip) LV-AO.

**TABLE 2**  
Estimation of Flow, Flow Variation, Partial Volume and Spillover Effects from Four Patients

Input	Shift (sec)	MBF (ml/g/min)		COV %	
		90 sec	330 sec	90 sec	330 sec
LA	0.0	1.18 ± 0.24	1.05 ± 0.33 <sup>†</sup>	20.0 ± 5.0	17.0 ± 2.6
0.53 ± 0.06	0.55 ± 0.05	0.18 ± 0.05	0.18 ± 0.05	—	—
LA-AO	1.55 ± 1.15	0.90 ± 0.40 <sup>†</sup>	0.95 ± 0.39 <sup>†</sup>	27.0 ± 6.0 <sup>†</sup>	16.0 ± 3.8 <sup>*</sup>

\*Parameters were obtained using either the initial 90 sec of the scan or with 330 sec of data.

<sup>†</sup>p < 0.05 when compared to values obtained using the unshifted left atrial (LA) input.

<sup>\*</sup>p < 0.05 when compared to values obtained using the 90 sec of data.

Abbreviations same as Table 1. Percent decrease in MBF = decrease in estimates of flow compared with those obtained with unshifted data.

### Effects of Scan Duration

To evaluate the effect of scan length on estimates of perfusion, mean flow was estimated from four patients with chest pain but angiographically normal coronary arteries

studied under resting conditions. Flow estimates yielded higher values when only the first 90 sec of data were used compared to when 5.5 min were used (1.18 ± 0.24 compared with 1.05 ± 0.33 ml/g/min, p < 0.05; Table 2). When the left atrial input was shifted to match either the aorta or the left ventricular inputs, the decrease in mean flow was not as large as when shorter scan lengths were used (11%

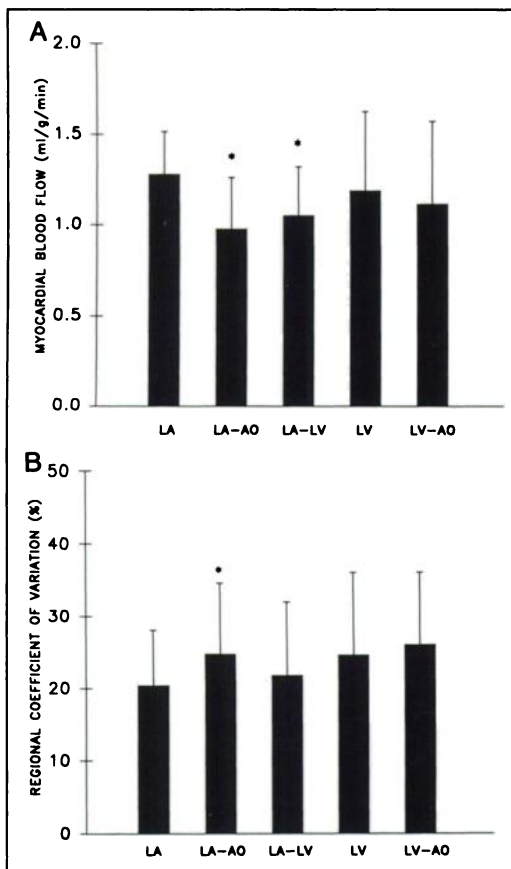


**FIGURE 3.** (A) Mean myocardial blood flow from 30 normal volunteers studied under baseline conditions using input curves obtained from the left atrial cavity (LA), the left atrial curve shifted in time to match either the ascending aorta curve (LA-AO) or the left ventricular curve (LA-LV); estimated from the left ventricular cavity (LV) without correction for time, and from the left ventricular curve shifted in time to match the ascending aorta curve (LV-AO). (B) Mean regional coefficient of variation corresponding to the baseline flows shown in (A). Slightly lower regional variability was obtained when either the LA or the LA-LV input curves were used. \*p < 0.05 compared with AO.

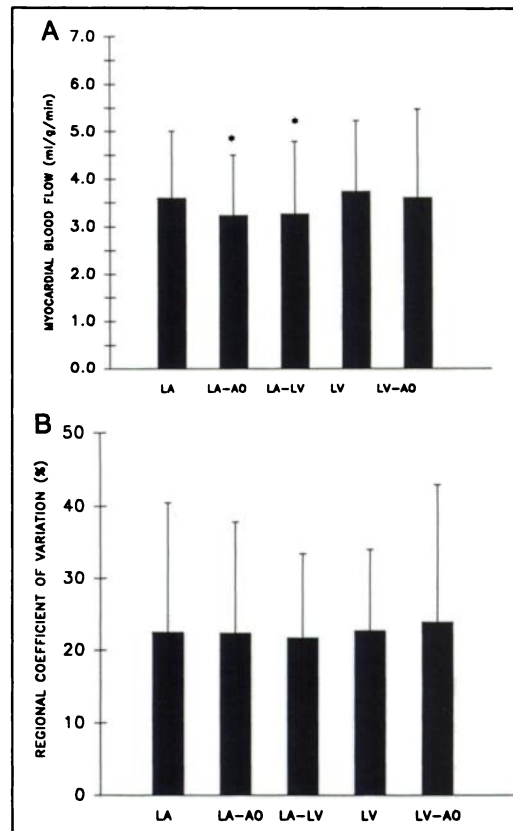


**FIGURE 4.** (A) Mean myocardial blood flow from the same 30 volunteers studied after intravenous dipyridamole using input curves obtained in the same fashion as those used under resting conditions. (B) Mean regional coefficient of variation of hyperemic flows corresponding to the flows shown in (A). Legends are the same as those in Figure 3. A similar pattern of changes in flow with the five different input functions was observed under hyperemic conditions as were obtained under resting conditions although the magnitude of the effects was more modest.

**TABLE 2**  
with Chest Pain and Angiographically Normal Coronary Arteries Studied Under Rest Conditions\*

Input	Shift (sec)	MBF (ml/g/min)		COV %	
		90 sec	330 sec	90 sec	330 sec
0.57 ± 0.08	0.57 ± 0.05	0.22 ± 0.03 <sup>†</sup>	0.22 ± 0.04 <sup>†</sup>	25.7 ± 19.5	10.9 ± 7.6 <sup>a</sup>
LA-LV	1.58 ± 1.18	0.90 ± 0.40 <sup>†</sup>	0.95 ± 0.39 <sup>†</sup>	26.0 ± 6.0 <sup>†</sup>	16.0 ± 4.0 <sup>†</sup>
0.57 ± 0.07	0.52 ± 0.05	0.22 ± 0.03 <sup>†</sup>	0.22 ± 0.04 <sup>†</sup>	25.9 ± 19.6	11.1 ± 8.0 <sup>†</sup>

± 8% compared with a 26% ± 20% decrease in flow,  $p < 0.001$ ; Table 2). In addition, the regional coefficient of variation of flow was less when the longer scans were used, and did not vary based on shifting of the input curve.

### Measurement of Dispersion

Table 3 summarizes the results of the computer simulations. Although shifting of the input function leads to a decrease in flow estimates and an increase in  $F_{MM}$  and  $F_{BM}$ , dispersion of the input curve of the same order of magnitude results in decreased  $F_{MM}$  and increased  $F_{BM}$  estimates but does not effect flow estimates.

### Correlation Between Estimated Parameters and Time Discrepancies

The tissue recovery coefficient ( $F_{MM}$ ) as well as the blood-to-tissue spillover fraction ( $F_{BM}$ ) were estimated along with myocardial flow within the mathematical model. Table 1 shows estimated  $F_{MM}$  and  $F_{BM}$  values for each of the five different input functions. The relationships between changes in flow,  $F_{MM}$ , and  $F_{BM}$  as a function of time shifts are shown in Figure 5. Under resting conditions, flow is inversely correlated with time shifts, while  $F_{MM}$  and  $F_{BM}$  are positively correlated. During hyperemia, flow and  $F_{MM}$  are inversely correlated with time shift while  $F_{BM}$  is positively correlated. While all three parameters are correlated with time shifts, under resting conditions, flow is the most sensitive parameter (Fig. 5A), while under hyperemic conditions,  $F_{BM}$  is most sensitive (Fig. 5B).

### DISCUSSION

Quantitation of myocardial perfusion with PET requires mathematical models which accurately describe the kinetic behavior of the tracers used and faithful measurements of radiotracer activity in blood and tissue. Although blood activity can be measured accurately by directly sampling blood from an artery, this approach is impractical for routine clinical use. In addition, the input function sampled directly from arterial blood although not subject to spillover or partial volume effects must be corrected for time delays and for dispersion. For routine clinical use, measurement of the input function from the reconstructed PET images is imperative.

The most appropriate sampling site to obtain arterial blood activity is at the level of the coronary ostia (i.e., the ascending aorta) since this is the point from which arterial blood irrigates the myocardial tissue. Thus, the input function obtained at this level provides the closest approxima-

tion of the actual time-tracer history for blood perfusing the myocardial bed. Nonetheless, measuring activity from a ROI placed within the ascending aorta is subject to errors due to the limited resolution of the current generation of tomographs, the small physical dimensions of the aorta, and potential contamination from adjacent vascular and myocardial structures.

Most investigators obtain the input function from a ROI placed within either the left atrial or the left ventricular cavity. Although placing a region with the left ventricular cavity is convenient, it is subject to motion artifact as well as spillover of radioactivity from myocardial tissue into the blood pool, especially problematic with extracted tracers such as  $^{82}\text{Rb}$ ,  $^{13}\text{NH}_3$  or  $^{62}\text{Cu}$ -PTSM. Although the input function obtained from a region placed within the left ventricular cavity can be corrected for effects of partial volume and spillover as recently described (18), we have previously demonstrated that radioactivity content obtained from a left atrial ROI most closely matches that obtained from direct arterial sampling (2). However, using computer simulations we have shown that time discrepancies between input and tissue curves lead to errors in estimates of flow, especially at low flows (5). Flow estimates made without correction for time discrepancies overestimate flow and the magnitude of this overestimation becomes more severe at lower flows. In this study, we evaluated the

**TABLE 3**  
Effect of Time Shift and Dispersion of the Input Function on Parameter Estimates

Shift (sec)	$F_{MM}$	$F_{BM}$	Flow (ml/g/min)	% Error in flow
0.3	0.701	0.203	1.00	0.0
0.6	0.705	0.192	1.00	0.0
1.0	0.688	0.248	0.86	14%
2.0	0.745	0.263	0.78	22%
$\tau$ (sec)				
0.3	0.700	0.210	1.00	0.0
0.6	0.691	0.214	1.00	0.0
1.0	0.676	0.218	1.00	0.0
2.0	0.621	0.227	1.00	0.0

Comparison of estimated  $F_{MM}$ ,  $F_{BM}$ , and flow values obtained from computer simulations where the input function defined as a gamma-variate (Equation 1) was shifted in time to estimated values obtained when the same input function was "dispersed" by the dispersion equation shown in Equation 2. The value of the simulated parameters are:  $F_{MM} = 0.7$ ,  $F_{BM} = 0.2$ , and flow = 1.0 ml/g;  $\tau$  = dispersion coefficient.

magnitude of time discrepancies between input curves obtained from the two ROIs that are typically used for myocardial studies and quantified the effect on estimates of flow.

Under baseline conditions, the input function appeared almost 1 sec earlier in the left atrial cavity than in the ascending aorta. As anticipated from the results of computer simulations (5), this earlier time of arrival was associated with a higher estimated flow. Nonetheless, the magnitude of the error in flow estimates is four to five times greater than that originally obtained (5). In our previous simulation studies, a 1-sec shift led to 4%–5% error in flow estimates for a simulated flow of 1.0 ml/g/min, while in the present study, a 1-sec shift between the left atrial cavity and aorta led to a 23% error in flow. This is due to differences in the shape of the input function. In the original error analysis we simulated the input function by a gamma variate function which had a FWHM of approximately 30 sec. The input function obtained in patient studies after a

bolus injection of  $^{15}\text{O}$ -water has a FWHM of only 15 sec. The greater the “spread” of the bolus, the less effect time discrepancies will have.

Since the time discrepancy between the left ventricular cavity and aorta was minimal (0.25 sec), estimates of flow obtained from a left ventricular input function corrected for time differences were not markedly effected by correcting the left ventricular curve for time. Nonetheless, as shown in Figure 1, the input function obtained from the left ventricle is contaminated by partial volume and spillover effects giving an inaccurate tracer content. This inaccuracy would be magnified using extracted flow tracers unless correction for myocardial to blood spillover is performed.

In addition to the above, the results of this study demonstrate that the duration of the scan will have important effects on flow estimates, estimates of regional variability and effects of time shifts. Longer scan durations led to lower flow estimates, decreased regional variation and less sensitivity to input time shifts compared to shorter scans. One potential explanation for these observations may be related to the weighting of data since shorter scans are weighted more heavily towards the early part of the tissue curve where spillover is greatest. Since flow and spillover are correlated, flow estimates are less stable. Further work will be necessary to evaluate whether increasing the scan length to achieve more stable estimates of flow with decreased sensitivity to time shifts impairs sensitivity to hyperemic flow rates (23).

To properly correct the left atrial input for time discrepancies, an accurate reference input curve is needed. In the present study we used two different reference curves obtained from the left ventricle and the ascending aorta. Differences in the shapes of the input and reference curves can lead to errors in estimated time differences. These differences in curve shapes can be due to a number of factors such as dispersion, spillover of activity from surrounding tissues into blood and motion artifacts. While dispersion and mixing of blood occurs in the peripheral circulation and one would not expect major discrepancies between an input curve obtained from the left atrial cavity and the same input curve obtained from either the left ventricular cavity or the ascending aorta, small changes in the shape of the curves due to dispersion cannot be excluded. Results obtained in five resting studies show negligible dispersion between the left atrial and the ascending aorta curves suggesting that differences in the dispersion of the input curves is not a major source of error in the estimation of the time shift and consequently of flow.

Furthermore, the results of computer simulations (Table 3) show that when myocardial flow is estimated using a three-parameter kinetic model after a bolus injection, dispersion of the input function has no effect on flow estimates.

In the present study, time differences were estimated independently. We chose not to include an extra parameter to estimate the time differences within the operational model because of the high correlation of time discrepancies

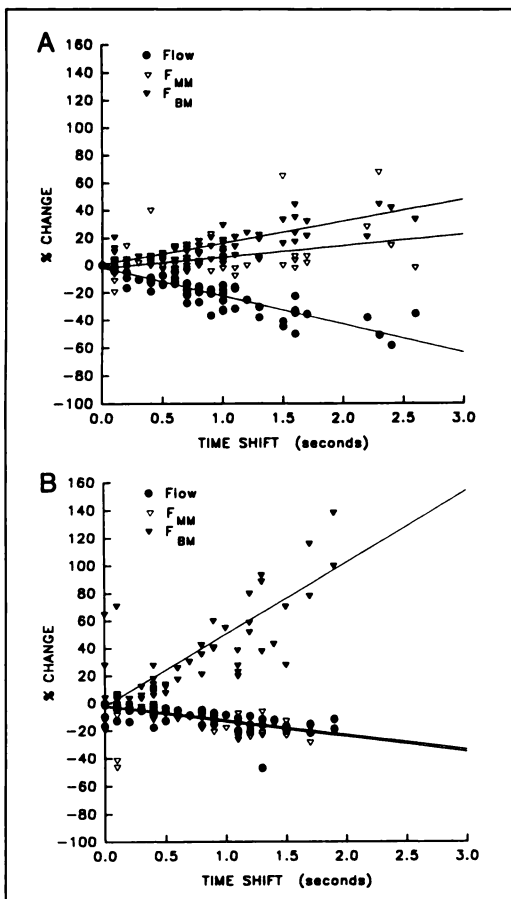


**FIGURE 5.** Correlations between changes in estimated parameters as a function of time shifts under resting conditions (A) and after dipyridamole (B). Under resting conditions, flow is inversely related to time shifts ( $y = -20.5 \times -1.8$ ,  $r = 0.91$ ) while  $F_{MM}$  and  $F_{BM}$  are positively correlated ( $y = 8.2 \times -2.2$ ,  $r = 0.41$  and  $y = 15.6 \times +0.6$ ,  $r = 0.85$ ). After dipyridamole, flow and  $F_{MM}$  are linearly and inversely related to the time shift ( $y = -10.5 \times -1.9$ ,  $r = 0.77$  and  $y = -10.8 \times -2.7$ ,  $r = 0.65$ , respectively) and  $F_{BM}$  is positively related ( $y = 52.0 \times -2.0$ ,  $r = 0.87$ ).

with the other parameters (flow,  $F_{MM}$ , and  $F_{BM}$ ) (Fig. 5). While estimation of the time shift within the kinetic flow model might simplify data analysis, implementation of this approach should be done cautiously only after scrutinizing the correlation and covariance matrices of the parameter estimates.

The entire 90 sec of dynamic data were used to estimate time differences between input curves. While it can be argued that most of the dynamic information is included in the early part of the curve, and that the use of the first 30–40 sec of data might lead to more reliable time estimates, we did not find significant differences in estimates of time differences using the first 40 sec of data versus using the entire 100 sec of data.

The results of the present study indicate that time discrepancies occur within measurements of the input curve obtained from either the left atrium or left ventricle and that these affect estimates of flow curves obtained. Low flow will be more sensitive to time discrepancies than higher flows, and sharper bolus injections will lead to greater error in flow estimates than more spreadout injections. In addition, although the aorta is preferable for use as a reference curve since it represents the region that is most temporally aligned with myocardial tissue, estimation of the time discrepancy between the left atrial and left ventricular curves can be used as an alternative if data from the ascending aorta is noisy, difficult to find, or not within the field of view. In addition, altered tracer administration protocols, such as use of constant infusions, may diminish the magnitude of time discrepancies but their use may be associated with other errors, such as decreased sensitivity to high flows (23).

## CONCLUSIONS

Time discrepancies between input curves and tissue curves lead to errors in flow estimates. The high sensitivity of flow estimates to time offsets precludes the use of an “average” shift. To accurately estimate myocardial perfusion using an input function obtained from the left atrial or left ventricular cavity, the proper time shift must be implemented. In addition, curves obtained from the left ventricle need to be corrected for myocardial motion and myocardial-to-blood spillover, especially when using extracted flow tracers. In the present study we estimated flow with  $^{15}\text{O}$ -water and a one-compartment kinetic model. Nonetheless, errors in flow estimates due to discrepancies between input and tissue curves are not unique to the use of any particular tracer or mathematical model. Estimates of flow, regional variability, and sensitivity to time shifts are dependent on the scan length as well. Thus, in order to estimate myocardial blood flow accurately with any given isotope or kinetic model, time discrepancies between input and tissue curves must be assessed and appropriate corrections implemented. Given this caveat, positron emission tomography provides the most accurate and reliable

noninvasive quantitation of myocardial perfusion in human subjects.

## ACKNOWLEDGMENTS

The authors thank Becky Leonard for preparation of the manuscript. Supported in part by National Institutes of Health Grant HL-17646, SCOR in Coronary and Vascular Disease, and Grant HL-46895, Optimization of PET Estimates of Myocardial Perfusion.

## REFERENCES

- Bergmann SR, Fox KAA, Rand AL, et al. Quantification of regional myocardial blood flow in vivo with  $\text{H}_2^{15}\text{O}$ . *Circulation* 1984;70:724–733.
- Bergmann SR, Herrero P, Markham J, Weinheimer CJ, Walsh MN. Noninvasive quantitation of myocardial blood flow in human subjects with oxygen-15-labeled water and positron emission tomography. *J Am Coll Cardiol* 1989;14:639–652.
- Huang SC, Schwaiger M, Carson RE, et al. Quantitative measurement of myocardial blood flow with oxygen-15 water and positron computed tomography: an assessment of potential and problems. *J Nucl Med* 1985;26:616–625.
- Iida H, Kanno I, Takahashi A, et al. Measurement of absolute myocardial blood flow with  $\text{H}_2^{15}\text{O}$  and dynamic positron-emission tomography. Strategy for quantification in relation to the partial-volume effect. *Circulation* 1988;78:104–115.
- Herrero P, Markham J, Bergmann SR. Quantitation of myocardial blood flow with  $\text{H}_2^{15}\text{O}$  and positron emission tomography: assessment and error analysis of a mathematical approach. *J Comp Assist Tomogr* 1989;13:862–873.
- Araujo LI, Lammertsma AA, Rhodes CG, et al. Noninvasive quantification of regional myocardial blood flow in coronary artery disease with oxygen-15-labeled carbon dioxide inhalation and positron emission tomography. *Circulation* 1991;83:875–885.
- Hutchins GD, Schwaiger M, Rosenspire KC, Krivokapich J, Schelbert H, Kuhl DE. Noninvasive quantification of regional blood flow in the human heart using N-13 ammonia and dynamic positron emission tomographic imaging. *J Am Coll Cardiol* 1990;15:1032–1042.
- Krivokapich J, Smith GT, Huang S-C, et al. Nitrogen-13-ammonia myocardial imaging at rest and with exercise in normal volunteers. *Circulation* 1989;80:1328–1337.
- Goldstein RA, Mullani NA, Marani SK, Fisher DJ, Gould KL, O'Brien HA Jr. Myocardial perfusion with rubidium-82. II. Effects of metabolic and pharmacologic interventions. *J Nucl Med* 1983;24:907–915.
- Wilson RA, Shea M, De Landsheere C, et al. Rubidium-82 myocardial uptake and extraction after transient ischemia: PET characteristics. *J Comp Assist Tomogr* 1987;11:60–66.
- Huang SC, Williams BA, Krivokapich J, Araujo L, Phelps ME, Schelbert HR. Rabbit myocardial  $^{82}\text{Rb}$  kinetics and a compartmental model for blood flow estimation. *Am J Physiol* 1989;256:H1156–H1164.
- Herrero P, Markham J, Shelton ME, Weinheimer CJ, Bergmann SR. Noninvasive quantitation of regional myocardial blood flow with rubidium-82 and positron emission tomography: exploration of a mathematical model. *Circulation* 1990;82:1377–1386.
- Herrero P, Markham J, Shelton ME, Bergmann SR. Implementation and evaluation of a two-compartment model for quantification of myocardial perfusion with rubidium-82 and positron emission tomography. *Circ Res* 1992;70:496–507.
- Herrero P, Markham J, Weinheimer C, et al. Quantification of regional myocardial perfusion with generator-produced  $^{62}\text{Cu}$ -PTSM and positron emission tomography. *Circulation* 1993;87:173–183.
- Bergmann SR, Herrero P, Anderson CJ, Welch MJ, Green MA. Measurement of regional myocardial perfusion in human subjects using  $^{62}\text{Cu}$ -PTSM [Abstract]. *J Nucl Med* 1992;33:837.
- Beanlands RSB, Muzik O, Mintun M, et al. The kinetics of copper-62-PTSM in the normal human heart. *J Nucl Med* 1992;33:684–690.
- Camicci P, Chiriatti G, Lorenzoni R, et al. Coronary vasodilation is impaired in both hypertrophied and nonhypertrophied myocardium of patients with hypertrophic cardiomyopathy: a study with nitrogen-13-ammonia and positron emission tomography. *J Am Coll Cardiol* 1991;17:879–886.
- Iida H, Rhodes CG, de Silva R, et al. Use of the left ventricular time activity curve as a noninvasive input function in dynamic oxygen-15-water positron emission tomography. *J Nucl Med* 1992;33:1669–1677.

19. Senneff MJ, Geltman EM, Bergmann SR. Noninvasive delineation of the effects of moderate aging on myocardial perfusion. *J Nucl Med* 1991;32:2037-2042.
20. Ficke DC, Beecher DE, Bergmann SR, Hoffman GR, Hood JT, Ter-Pogossian MM. Performance characterization of a whole body PET system designed for dynamic cardiac imaging. *IEEE* 1991;3:1635-1638.
21. Iida H, Kanno S, Miura M, Murakami M, Takahashi K, Uemura K. Error analysis of a quantitative cerebral blood flow measurement using  $H_2^{15}O$  autoradiography and positron emission tomography, with respect to dispersion of the input function. *J Cereb Blood Flow Metab* 1986;6:536-545.
22. Meyer E. Simultaneous correction for tracer arrival delay and dispersion in CBF measurements by the  $H_2^{15}O$  autoradiographic method and dynamic PET. *J Nucl Med* 1989;30:1069-1078.
23. Hack S, Eichling JO, Bergmann SR, Sobel BE. External quantification of myocardial perfusion by exponential infusion of positron emitting radionuclides. *J Clin Invest* 1980;66:918-927.

---

## ***Condensed from 15 Years Ago:***

### **Validity of Left Ventricular Ejection Fractions Measured at Rest and Peak Exercise By Equilibrium Radionuclide Angiography Using Short Acquisition Times**

**Matthias E. Pfisterer, Donald R. Ricci, Gerhard Schuler, Sue S. Swanson, Donald G. Gordon, Kirk E. Peterson and William L. Ashburn**

*University of California Medical Center, San Diego, California*

To validate ejection fraction (EF) calculations from 5 and 2 min of multiple-gated equilibrium radionuclide angiographic data and to establish its utility during alterations in cardiac performance, we studied 38 patients with chest pain suggestive of coronary artery disease. Twenty-four patients underwent contrast ventriculography (CV) as well as first-pass (FP) and equilibrium (EQ) radionuclide angiography at

rest, and 14 additional patients had both radionuclide tests performed at rest as well as during peak supine bicycle exercise. The resting 5-min acquisition ejection fractions were compared between each method and the following correlations were generated:  $r = 0.92$ ,  $n = 24$  (CV-EQ),  $r = 0.92$ ,  $n = 24$  (CV-FP), and  $r = 0.95$ ,  $n = 38$  (FP-EQ). The variability of EQ-EF calculations between two independent observers was  $< 2\%$ ; the mean absolute difference between two sequential 2-min acquisitions and the 5-min recordings was  $-0.1\% \pm 1.6\%$ , and the reproducibility of sequential 2-min ejection fractions was excellent ( $r = 0.98$ ). EQ and FP ejection fractions at symptom-limited exercise correlated well ( $r = 0.96$ ,  $n = 14$ ). We conclude that equilibrium radionuclide angiography is a valid method to measure EF both at rest as well as during peak exercise even when 2-min acquisition periods are used.

**J Nucl Med 1979; 20:484-490**